Payri, R.; Salvador Rubio, FJ.; Gimeno, J.; Venegas Pereira, OH. (2013). Study of cavitation phenomenon using different fuels in a transparent nozzle by hydraulic characterization and visualization. Experimental Thermal and Fluid Science. 44:235-244. doi:10.1016/j.expthermflusci.2012.06.013.

Study of Cavitation Phenomenon Using Different Fuels in a Transparent Nozzle by Hydraulic Characterization and Visualization

R. Payri, F.J. Salvador, J. Gimeno, O. Venegas

CMT-Motores Térmicos. Universidad Politécnica de Valencia, Camino de Vera s/n, Valencia, Spain.

ABSTRACT

In this paper the behavior of the internal flow under cavitating conditions and the influence of using different fuels is studied. For this purpose, a transparent nozzle (quartz plate) with a cylindrical orifice and four different fuels are used. The nozzle is installed in a pressurized rig with fuel in order to measure the mass flow and observe the flow inside the orifice using a special visualization technique with all fuels. Since the refractive index of the vapor bubbles of the fuel is different to de refractive index of the fuel in liquid state, the cavitation inside the nozzle can be appreciated. Pressure conditions at which the first bubbles inside the orifice appear are compared with the pressure conditions for mass flow collapse, showing that the beginning of the cavitation occurs before the mass flow collapse and that it depends both on the upstream and downstream pressure conditions and on the fluid viscosity used. Additionally it is observed that the mass flow collapse takes place once the cavitation is fully developed through the whole orifice and the presence of bubbles in the spray before the mass flow collapse indicating that the cavitation appears before the mentioned collapse.

HIGHLIGHTS

> Visualization of cavitation phenomenon in transparent diesel injection nozzles. > Influence of using different fuels in cavitation phenomenon. > Fuels with less viscosity tend to cavitate sooner. > Incipient cavitation occurs before the mass flow collapse. > The first bubbles in the spray appear before the mass flow collapse occurs.

KEYWORDS: cavitation, transparent nozzle, diesel, visualization.

1. INTRODUCTION

The reduction of emissions and fuel consumption is currently one of the most important subjects in the automotive sector and society in general. The number of research activities focused on the fundamental understanding of the internal combustion engine processes has increased rapidly.

http://dx.doi.org/10.1016/j.expthermflusci.2012.06.013, Experimental Thermal and Fluid Science 44 (2013) 235–244

One of the areas of interest in diesel engines is the study of nozzle flow behavior in fuel injectors. As it is well known through previous studies from other authors [1-7], the flow behavior inside the orifice is strongly related to the behavior of the spray at the exit and its interaction with the air, affecting the mixing and combustion process. They have analyzed the influence of cavitation inside the discharge orifice on atomization process and consequently on spray characteristics.

Many researchers have worked with diverse visualization techniques of the spray at the exit of the nozzle under non cavitating conditions to obtain information about the characteristic parameters of the spray, such as the angle and penetration. However, cavitation phenomenon has been revealed to play an important role in high pressure systems; so, other researches [8-18] point to the visualization of the flow inside the nozzle with the goal to observe the cavitation phenomenon and its influence in the spray development. Thereby, different nozzle models have been developed with optical materials that allow the visualization inside the hole such as quartz and methacrylate.

Some studies were performed with planar nozzles in order to better see the cavitation [8-11] and others with large-scale cylindrical nozzle [12-15] to facilitate the visualization of the phenomenon; however, there are few researches which focus on studying experimentally the phenomenon of cavitation in diesel injection orifices of smaller scale or real size [15-18]. With all this knowledge and using a small scale model and different fuels, this work targets to link the mass flow collapse with the cavitation inside the orifice and to define a new cavitation criterion.

Hydraulic criterion to detect the start of cavitation based on the start of mass flow choking has been used traditionally. Nevertheless, a few studies made with transparent orifices revealed that cavitation bubbles appear at less critical conditions [10; 11]. One of the goals of this paper is to know the behavior of the cavitation in a transparent nozzle (quartz-fused silica, SiO_2) performing a study to determine the cavitation inception using different fuels to determine the effect of its properties in the appearance of cavitation and to provide a wider range of validity to the results. To do so, hydraulic characterization in terms of mass flow is made for all fuels, finding the pressure conditions where mass flow chokes and including correlations for discharge coefficient both in cavitating and non-cavitating conditions. Simultaneously, visualization in a pressurized chamber is performed to link the hydraulic behavior measures and visualization to provide a new criterion to determine the start of cavitation and compare it with the traditional criterion (collapse of the mass flow).

For the visualization a special optical system and flash (white light) backlighting has been developed to focus a window size of 3mm (around 500 pixel/mm) that allows seeing the flow inside the orifice and a portion of the spray at the exit (first 1.5 mm of the spray). Discharge chamber is filled with the same liquid that is injected, so that cavitation bubbles present both inside and at the exit of the orifice can be observed. This kind of images make possible the analysis of two different phenomena related to cavitation process. Firstly, the cavitation inception determination and, secondly, these images can be compared with hydraulic characterization results in order to know what happens inside the orifice when the flow collapses.

To carry out the tests, the following fuels are used: n-heptane, n-decane, n-dodecane and commercial diesel. Besides, a visualization test rig is used to make the hydraulic characterization and the visualization simultaneously.

This paper is structured in four sections. First, a review of the concepts used in the calculation and definition of the cavitation and internal flow in nozzles is made introducing several important parameters that will be used in the rest of the study. Second, the experimental facilities and methodology are described, paying special attention to the optical system for internal flow visualization. In the third section, results from hydraulic characterization and internal flow visualization are shown and analyzed, trying to explore the relationship between flow parameters and cavitation development. Finally, some general conclusions and possible future works will be established.

2. THEORETICAL BACKGROUND

In a diesel injector nozzle, high velocities at the orifice inlet due to the abrupt change of section and flow direction tend to separate the boundary layer from the wall at the inlet section. This causes a flow contraction which allows the static pressure to fall under vapor pressure of the working fluid, leading to a local change of state from liquid to vapor. This phenomenon is called cavitation.

As a consequence of the complexity to obtain information about the behavior of the flow inside the orifice in real nozzles, non-intrusive techniques have been developed to determine the appearance of the cavitation. One of the criteria often used to determine the appearance of the cavitation is the one proposed by Nurick [19], where the mass flow obtained in stationary conditions increases as a linear function of the square root of the pressure drop until a point where it stabilizes due to the cavitation phenomena. At this point, the so called ‘‘choked flow” occurs and pressure conditions needed to achieve this situation are named critical cavitation conditions (Figure 1).

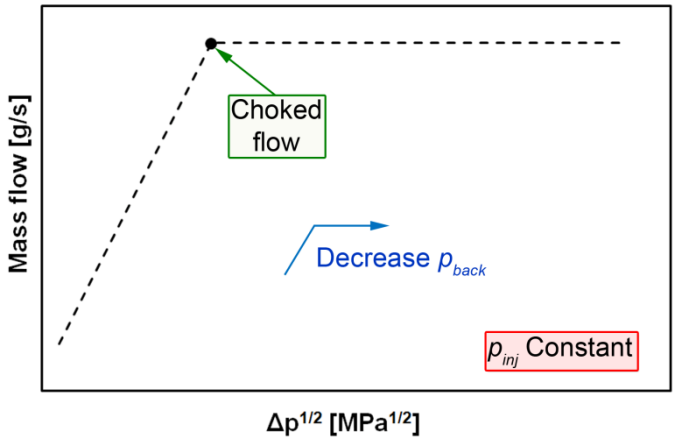

Figure 1. Mass flow rate through cavitating nozzles (p_{inj} constant, varying p_{back}).

This situation of choked flow affects directly the discharge coefficient (C_d). This parameter is defined as the relation between real and theoretical (given by Bernoulli's equation) mass flow as shown in Equation (1).

$$C_d = \frac{\dot{m}}{A_0 \cdot (2 \cdot \rho_f \cdot \Delta p)^{1/2}} \quad (1)$$

where $\dot{m}$ is fuel mass flow at stationary conditions, A_0 the outlet geometrical area of the orifice, ρ_f the fuel density and $\Delta p = p_{inj} - p_{back}$ is the pressure drop. In non-cavitating conditions, the discharge coefficient is function of the Reynolds number [1, 5-7, 20]; however, when the flow begins to cavitate the discharge coefficient depends mainly on cavitation number (K) as shown in Equation (2) analyzed by Nurick [19] in his unidimensional model.

$$C_d = C_c \cdot K^{1/2} \quad (2)$$

The cavitation number (K) defined by Nurick (Equation (3)). This K increases as the rail pressure (p_{inj}) decreases or when the discharge pressure downstream the orifice (p_{back}) increases. p_v is the vapor pressure of the fuel. As the cavitation number (K) is smaller, the higher tendency to cavitate.

$$K = \frac{p_{inj} - p_v}{p_{inj} - p_{back}} \quad (3)$$

This way both mass flow choking and reduction in discharge coefficient are indirect methods to predict at which conditions the cavitation appears in a nozzle. However, other authors have tried to go one step further in understanding the phenomenon of cavitation and its appearance inside the orifice. For most of these researches several models for transparent nozzles at large scale have been used [12-18], others have used geometries at smaller scale but that do not keep up to the exact geometry of a real nozzle [2, 3, 21] and very few have performed studies in nozzles at small scale and/or with reproducible geometry [22]. Some of these studies, along with others where transparent nozzles have not been used [7] have demonstrated that cavitation inception detected by visualizing bubbles in the nozzles is not coincident with the collapse of mass flow.

3. EXPERIMENTAL SET UP

To carry out the hydraulic characterization of the nozzle and flow visualization inside it, a rig as the one shown in Figure 2 has been used. This rig consists of a stainless steel vessel, including two opposed optical windows, so that backlighting visualization can be performed. The upper cap allows the fuel supply and is adapted to contain the transparent nozzle. The bottom cap includes the backpressure regulation system.

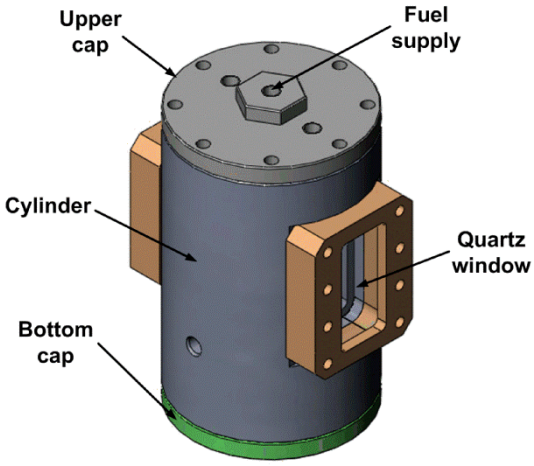

Figure 2. Visualization test rig.

The transparent nozzle is made of fused silica SiO_2 and has an exit diameter of 510um and 1mm length (Figure 3 and Figure 4).

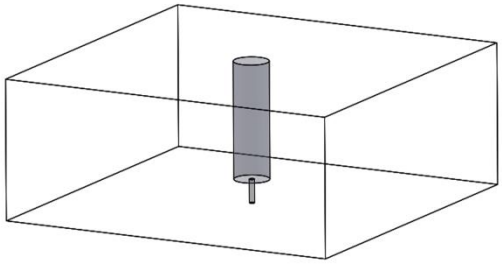

Figure 3. Transparent nozzle.

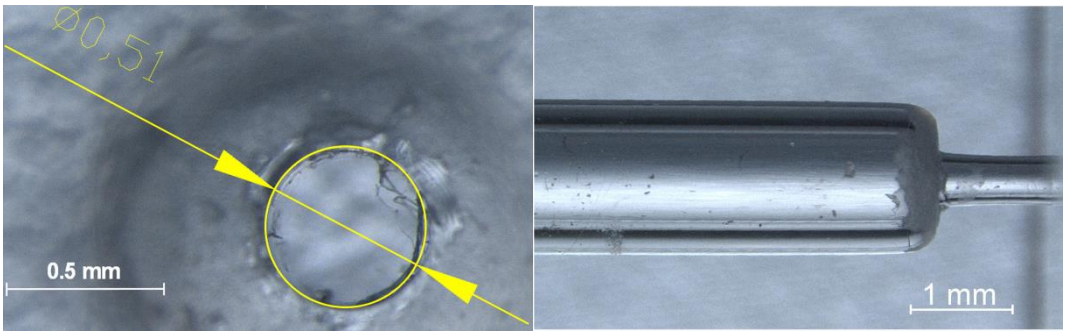

Figure 4. Transparent nozzle images obtained with microscopy.

For the assembly of the nozzle in the rig, a holding system has been developed as shown in Figure 5. It consists of an upper cap coupled directly to the rig cylinder and allows the fuel supply; besides it has a lower piece called “base” that allows the entry of light for flow visualization and finally it has a large size nut which couples the two

pieces (upper cap and base). The transparent nozzle is located in the middle of the cap and the base and is separated by expanded graphite laminated gaskets to prevent fuel leakage and local strains over quartz surfaces in contact that may lead to a breakage of the nozzle.

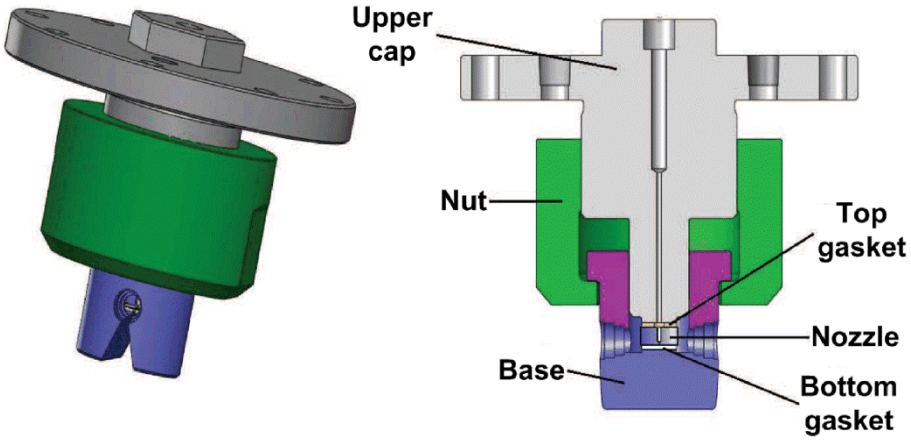

Figure 5. Holding system for the transparent nozzle.

All the experiments developed for this article are made with a fuel-filled chamber so that it is pressurized governing the flow that gets out of the rig and the fuel supply system is a conventional common rail. Each fuel is tested at its maximum reachable rail pressure and a discharge pressure scanning is done. The fuels used are n-heptane, n-decane, n-dodecane and commercial diesel fuel; Table 1 presents a summary of the properties considered in this study. The refractive index of the quartz plate is 1.463 at a wavelength of 486nm [23, 24] and according to Table 1 [0] the fuel that is closer to this value is commercial gasoil which is expected to produce images with higher quality than others.

Fuel	Density$_{@40^oC}$ [Kg/m3]	Viscosity$_{@40^oC}$ [cSt]	Vapor pressure$_{@40^oC}$ [MPa]	Refractive index [-]
n-heptane	666.93	0.49	0.012	1.387
n-decane	715.10	0.96	0.00049	1.417
n-dodecane	734.77	1.5	0.000058	1.427
Commercial diesel	826.44	2.6	Negligible	1.483

Table 1. Physical properties of the fuels.

3.1 Hydraulic characterization

Hydraulic characterization is done by measuring the mass flow of the nozzle injecting fuel at stationary conditions. For this purpose, the test rig is filled with fuel and the nozzle injects in continuous flow. A valve placed at the test rig exit regulates the pressure inside it. Once the target chamber pressure value is reached, the valve is opened so that the flow that gets out from the chamber is equal to the flow through the orifice at each instant. This way, measuring the mass that escapes the test rig (with a gravimetric balance) for a given time, the stationary mass flow can be calculated. Mass flow is measured for different conditions of discharge

pressures, from 0.1 to 1.5 MPa, for each fuel. Figure 6 shows a diagram of the assembly used for the measures of mass flow in continuous (permeability).

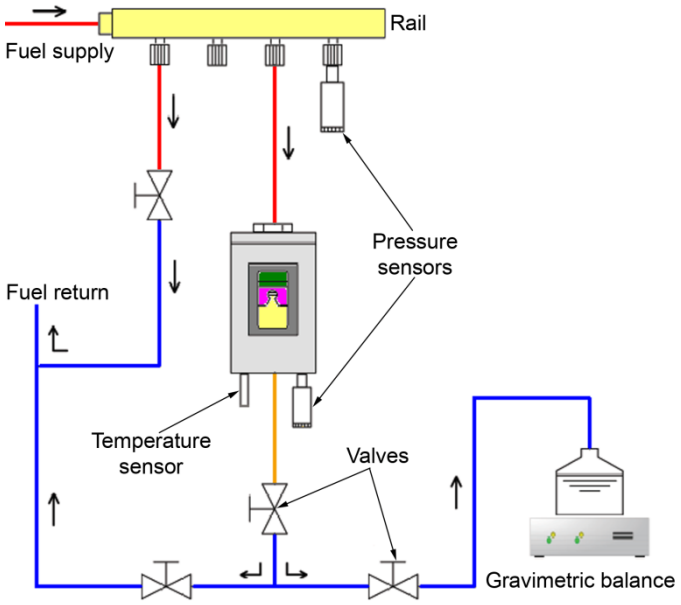

Figure 6. Scheme for the hydraulic characterization.

3.2 Internal flow visualization

The optical system developed for this purpose includes two optical fibers, a PCO SensiCam CCD Camera and one optical lens, aligned between each other in order to reach high zoom levels. These elements are placed in a three-axis coordinate system (Figure 7).

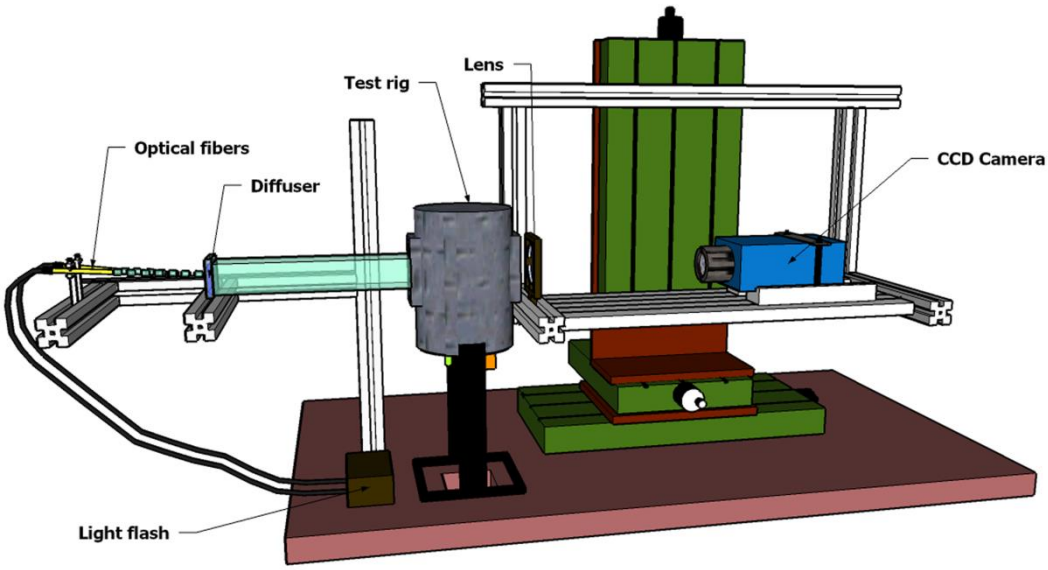

Figure 7. Three-axis coordinate system for visualization.

This configuration allows fixing distances between test rig, focal lens and camera so that visualization window and zoom level can be adapted to the objective of the experiments and in functions of the fuel used keeping the same window size. In this paper, all the images are obtained at a resolution of 1280X1024 pixels, 1μs of exposure time and 3mm of window size with the goal to observe the cavitation inside the orifice and part of the spray at the exit. Additionally, an optical diffuser is placed after light flash exit. This element diffuses the flash light and produces a uniform illumination in the chamber region under study. Figure 8 shows a diagram of the acquisition system used for visualization.

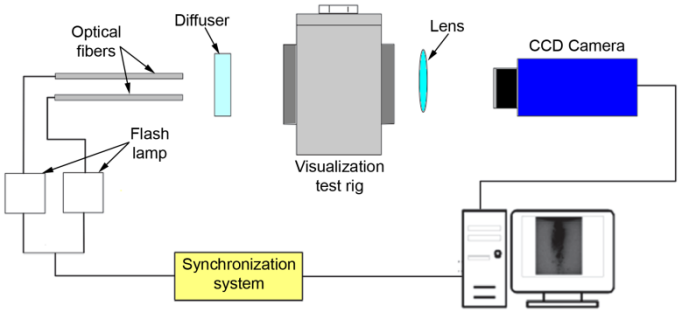

Figure 8. Scheme of the synchronization system.

Once the hydraulic characterization for all fuels has been made, the images of the flow inside the orifice and part of the spray at the exit are obtained using diffused backlighting illumination. Due to the difference in refractive index between liquid and vapor phase, only bubbles inside the orifice and those coming out of it are visualized. The same discharge pressures intervals from hydraulic characterization are used (from 0.1 to 1.5 MPa) and 100 images per test condition are taken. However, for visualization tests some additional backpressure values are added in order to obtain images of the cavitation appearance and its development inside the orifice.

In order to detect better the cavitating zones inside the orifice as well as bubbles in the spray at the exit of the orifice, the images obtained are posteriorly processed with a custom-made algorithm. This function allows to match in position each image with respect to the background; which is later subtracted.

4. RESULTS AND DISCUSSION

4.1 Hydraulic characterization

Once determined the real diameter of the orifice using a microscope (Figure 4), the measures of mass flow rate were made under stationary conditions at different backpressure values keeping rail pressure constant (maximum rail pressure for each fuel). By applying a linear fit to the first points of the curve and calculating the intersection with the value of mass flow after choking, critical conditions can be obtained [5]. This information is shown in the Figure 9 and the values of critical cavitation number (K_{crit}) are tabulated in Table 2.

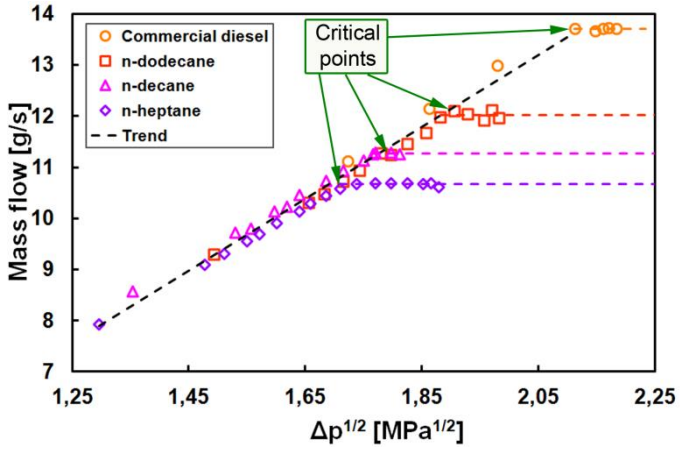

Figure 9. Mass flow behavior.

It can be observed in Figure 9 that the mass flow choke for each fuel occurs at different values of the square root of the pressure drop ($\Delta p^{1/2}$). The dashed lines show the tendency for each fuel. Under non-cavitating conditions this tendency is linear to the root of the pressure drop and all tested fit that slope[1]. However, when the flow collapses the tendency of each fuel changes at a different level of mass flow.

Fuel	p_{inj} [MPa]	$\Delta p_{crit}^{1/2}$ [MPa$^{1/2}$]	K_{crit}
n-heptane	3.6	1.71	1.22
n-decane	3.7	1.77	1.20
n-dodecane	4.2	1.88	1.18
Commercial diesel	4.8	2.12	1.07

Table 2. Critical cavitation number for each fuel.

Knowing the geometry of the nozzle, the density of the fuels and using Equation (1) is possible to obtain the discharge coefficient for each fuel and all tested conditions. Figure 10 shows the evolution of the discharge coefficient in function of Reynolds number. It can be observed that the discharge coefficient increases continuously with Reynolds number and has an asymptotic maximum value for non-cavitating conditions.

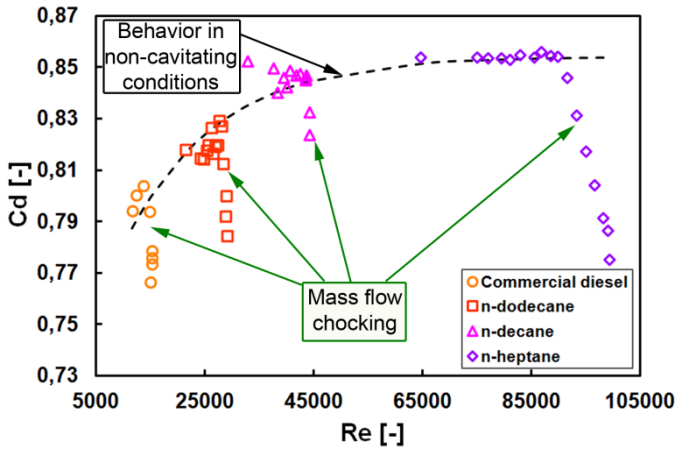

Figure 10. Cd against Re.

[1] Although for each fuel the slope varies a little, not all the lines were drawn in order to facilitate understanding the figure.

From data obtained in non-cavitating conditions for each fuel, a correlation can be obtained for the discharge coefficient in function of Reynolds number as shown in Equation (4).

$$C_d = A \cdot Tanh\left(\frac{Re+C}{B}\right) \quad (4)$$

where A, B and C are the correlation coefficients and they are tabulated in Table 3.

Coefficients	Value
A	0.85
B	32961.1
C	41128

Table 3. Coefficients of Equation (4).

However, when the nozzle is cavitating, discharge coefficient experiences a decrease. This decrease is directly related to the mass flow collapse observed in Figure 9. As mentioned before, at cavitating conditions the discharge coefficient depends mainly on the cavitation number (K) and is linearly related to the root of the cavitation number (Equation (2)). Figure 11 shows the behavior of the discharge coefficient in function of the square root of the cavitation number for each fuel.

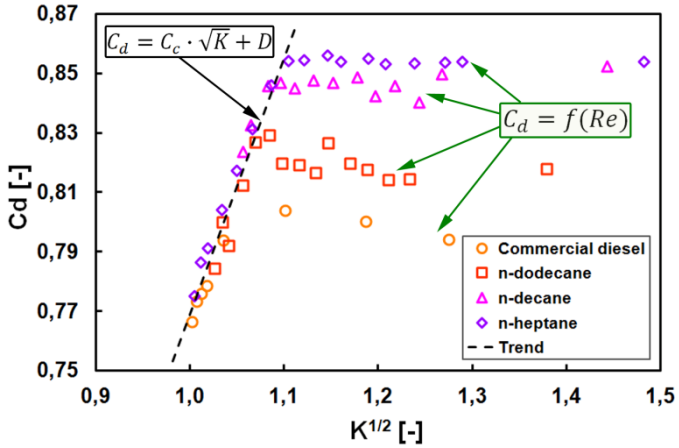

Figure 11. Discharge coefficient as a function of $K^{1/2}$.

Equaling Equation (2) and Equation (4) a new expression relating the critical cavitation number with Reynolds number (Equation (5), Figure 12) is obtained:

$$K_{crit} = \left[\frac{A \cdot Tanh\left(\frac{Re+C}{B}\right) - D}{C_c}\right]^2 \quad (5)$$

where D is the intersection point with the Y axis (Figure 11). The values for C_c and D are tabulated in Table 4.

Coefficients	Value
C_c	0.86
D	0.09

Table 4. Coefficients of Equation (5).

It can be observed that the critical points obtained in the four fuels are on the same tendency line given by Equation (5) and shown in Figure 12. It is important to take into account that the change in Reynolds number depends not only on the pressure drop but also on the physical properties of each fuel as shown in Equation (6).

$$Re = \frac{D_0 \cdot U_{th}}{\nu_f} = \frac{D_0 \cdot (2 \cdot \Delta p)^{1/2}}{\rho_f{}^{1/2} \cdot \nu_f} \quad (6)$$

where D_0 is the exit diameter of the orifice, ρ_f and ν_f are density and kinematic viscosity of the fuel respectively and Δp the pressure drop. In Figure 13 can be observed that the increase in K_{crit} is due partly to the pressure drop but mainly to the fuel properties strictly speaking. It is important to take into account that for all tests the maximum injection pressure reachable for each fuel (Table 2) was used and that this value also depends on the fuel properties.

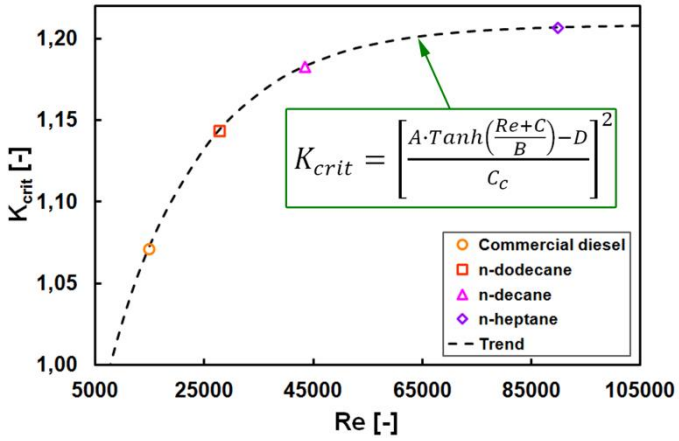

Figure 12. Critical cavitation number vs. Reynolds number.

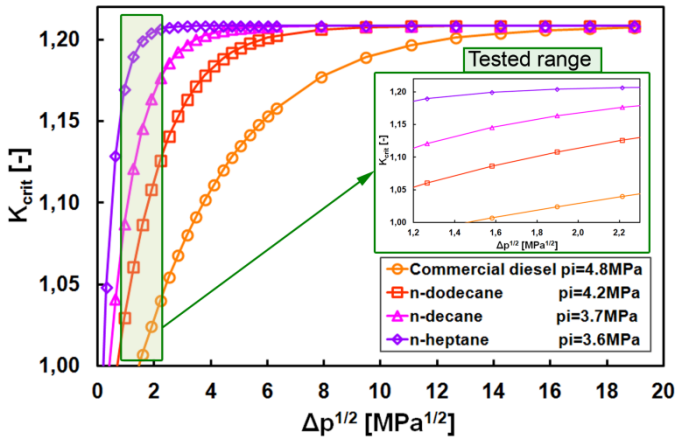

Figure 13. Critical cavitation number vs. square root of pressure drop.

In Figure 13 can be observed that the fluid with less viscosity (n-heptane) has a steeper slope which makes it cavitate before all other fuels independently of the square root of the pressure drop. In the same way it is observed that as the fuels are more viscous the slope decreases and the K_{crit} is lower.

The explanation to the flow behavior using different fuels is that a fluid with higher viscosity generates a higher pressure drop through the orifice, which causes that the pressure where the contraction at the orifice inlet occurs (Figure 14) is higher as well and therefore the fluid needs more critical conditions to cavitate.

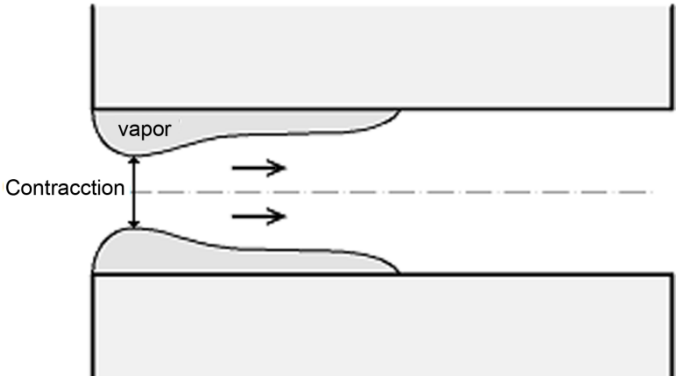

Figure 14. Contraction at the orifice inlet.

Thus, these results have allowed knowing the cavitation inception taking as criteria the flow collapse and the behavior of the discharge coefficient and the critical cavitation number for each fuel. Besides, observing Figure 10, Figure 11 and Figure 12, which are plotted with adimensional numbers (Re and K), it can be concluded that the conditions in the nozzle do not depend on the fuel that passes through the orifice. Next, the results obtained in visualization tests are shown.

4.2 Internal flow visualization

Once the hydraulic characterization has been done and the cavitation inception determined using as criterion the mass flow collapse we proceed to visualize the flow inside the orifice. Figure 15 shows an image that represents an average of the 100 images taken for a measure condition. In this image is not possible to appreciate the real shape of the bubbles because the exposure time is not small enough to freeze the image (1μs); however, its behavior at different conditions can be appreciated (Figure 16).

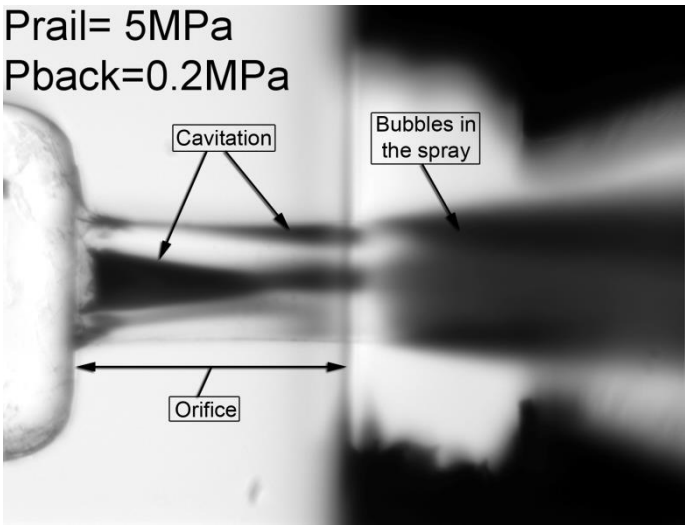

Figure 15. Average image for commercial diesel at $p_{inj} = 5\text{MPa}$ and $p_{back} = 0.2\text{MPa}$.

Figure 15 shows the cavitation inside the orifice and the bubbles in the spray at the exit (dark zone). On the other hand, Figure 16 shows the evolution of cavitation for commercial diesel as the discharge pressure downstream the orifice changes. For each condition, the figure on the right shows the image without background in order to appreciate better the zones of higher and lower cavitation.

Being a circular orifice instead of flat as in other studies [9], the images in Figure 16 show the cavitation around the whole wall of the orifice. Thus the cavitation observed in the central part of the orifice represents the cavitation from both the front and back of the orifice.

When comparing the results of hydraulic characterization with those from visualization, it is observed that the incipient cavitation occurs at a pressure differential lower than when the mass flow collapse occurs ($\mathbf{1.84MPa^{1/2} < 2.12MPa^{1/2}}$) or at higher cavitation numbers ($\mathbf{1.42 > 1.07}$); which confirms the results obtained in other studies [7].

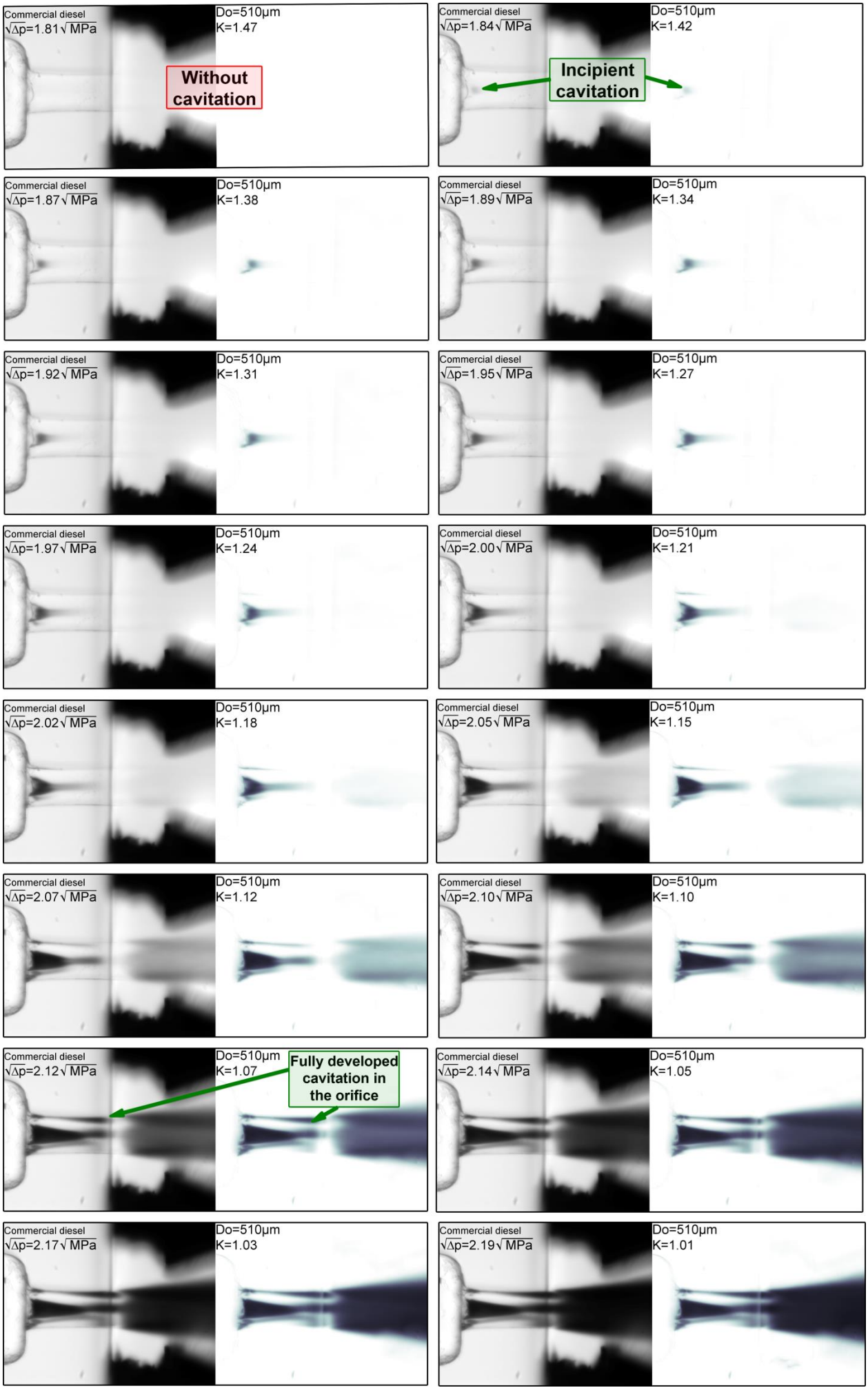
Commercial diesel
√Δp=1.81√MPa
Do=510μm
K=1.47
Without cavitation
Commercial diesel
√Δp=1.84√MPa
Do=510μm
K=1.42
Incipient cavitation
Commercial diesel
√Δp=1.87√MPa
Do=510μm
K=1.38
Commercial diesel
√Δp=1.89√MPa
Do=510μm
K=1.34
Commercial diesel
√Δp=1.92√MPa
Do=510μm
K=1.31
Commercial diesel
√Δp=1.95√MPa
Do=510μm
K=1.27
Commercial diesel
√Δp=1.97√MPa
Do=510μm
K=1.24
Commercial diesel
√Δp=2.00√MPa
Do=510μm
K=1.21
Commercial diesel
√Δp=2.02√MPa
Do=510μm
K=1.18
Commercial diesel
√Δp=2.05√MPa
Do=510μm
K=1.15
Commercial diesel
√Δp=2.07√MPa
Do=510μm
K=1.12
Commercial diesel
√Δp=2.10√MPa
Do=510μm
K=1.10
Commercial diesel
√Δp=2.12√MPa
Do=510μm
K=1.07
Fully developed cavitation in the orifice
Commercial diesel
√Δp=2.14√MPa
Do=510μm
K=1.05
Commercial diesel
√Δp=2.17√MPa
Do=510μm
K=1.03
Commercial diesel
√Δp=2.19√MPa
Do=510μm
K=1.01

Figure 16. Evolution of cavitation for commercial diesel at different discharge pressures.

Besides, the critical pressure drop for all fuels (choked mass) matches the pressure drop when cavitation is fully developed in the orifice as shown in Figure 16 (i.e. $\Delta \boldsymbol{p^{1/2}} = \mathbf{2.12MPa^{1/2}}$ for commercial diesel), which demonstrates that the mass flow collapse occurs once the cavitation extents up to the orifice exit (Figure 16). Besides, it is observed that before the collapse occurs there is already presence of bubbles in the spray (Figure 17) as shown in other studies [7]. The same analysis is done for the other three fuels and they show the same behavior as commercial diesel, although for different values of the pressure differential.

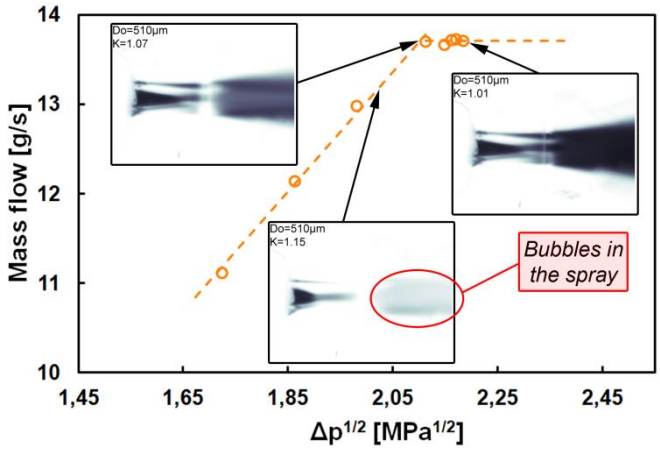

Figure 17. Comparison of visualization images and mass flow measurements for commercial diesel.

This way, a new critical cavitation number can be defined taking the incipient cavitation criterion; that is, when cavitation first appears inside the orifice ($\boldsymbol{K_{crit-incipient}}$). For all tested fuels the $\boldsymbol{K_{crit-incipient}}$ is bigger than the $\boldsymbol{K_{crit}}$ found in hydraulic characterization as shown in Table 5.

Fuel	K_{crit}	$\Delta p_{crit}^{1/2}$ [MPa$^{1/2}$]	$K_{crit-incipient}$	$\Delta p_{crit-incipient}^{1/2}$ [MPa$^{1/2}$]
n-heptane	1.22	1.71	1.60	1.49
n-decane	1.20	1.77	1.61	1.52
n-dodecane	1.18	1.88	1.52	1.65
Commercial diesel	1.07	2.12	1.42	1.84

Table 5. Comparison between K_{crit} and $K_{crit-incipient}$

Figure 18 shows a comparison of images of the four fuels right when cavitation appears (incipient cavitation). It is observed that the fuel with minor viscosity (n-heptane) cavitates at less critical conditions and commercial diesel, which has a higher viscosity, needs more critical conditions to cavitate. This behavior is the same obtained in hydraulic characterization, the collapse occurred first in n-heptane and last in commercial diesel (Figure 9).

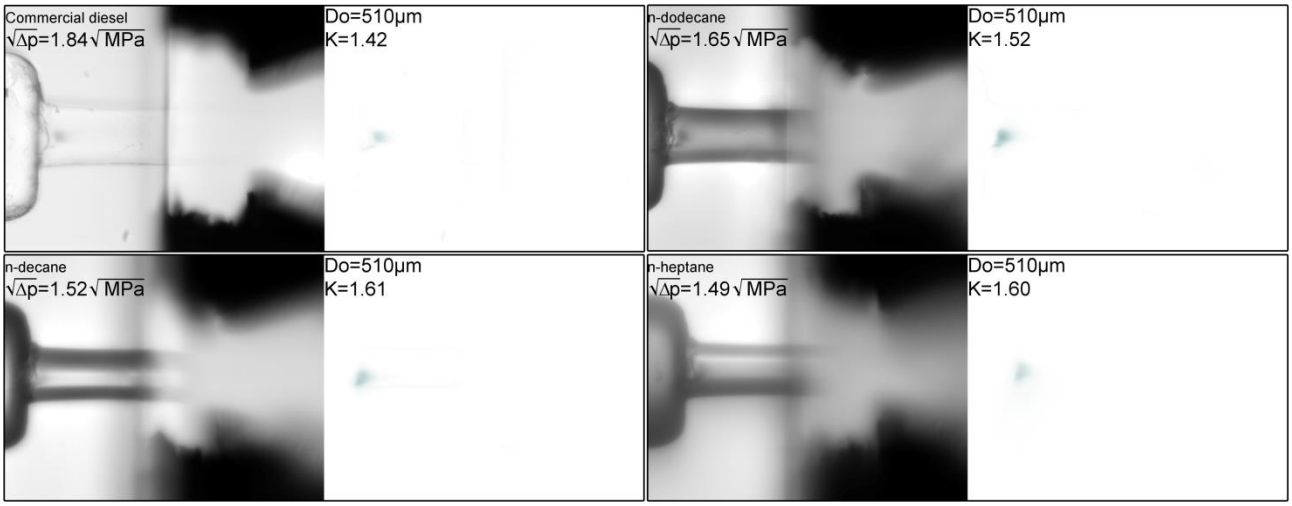

Figure 18. Incipient cavitation for all fuels.

The influence of the refractive index in the image quality can also be observed. The fuel with more similar refractive index to the quartz refractive index (in this case commercial gasoil) allows obtaining images of higher quality than those obtained with fuels whose refractive indexes (see Table 1) are more different to quartz refractive index; for instance with n-heptane the orifice borders look very thick and cannot be distinguished from the cavitation inside the orifice (see Figure 18, n-heptane graphic), making more difficult to process the images. To match the refractive index of the fuels with the refractive index of the quartz doping fluids can be used. However, in this study none of the fuels were doped on purpose in order to maintain their physical properties and be able to appreciate the influence of pure fuels on cavitation.

With the results obtained in visualization tests it has been demonstrated that the cavitation inception happens at a cavitation number higher to the one where the collapse occurs (Figure 19). Besides, it has been seen that once cavitation is fully developed inside the orifice the mass flow collapses and that the bubbles present in the spray appear before the flow collapse.

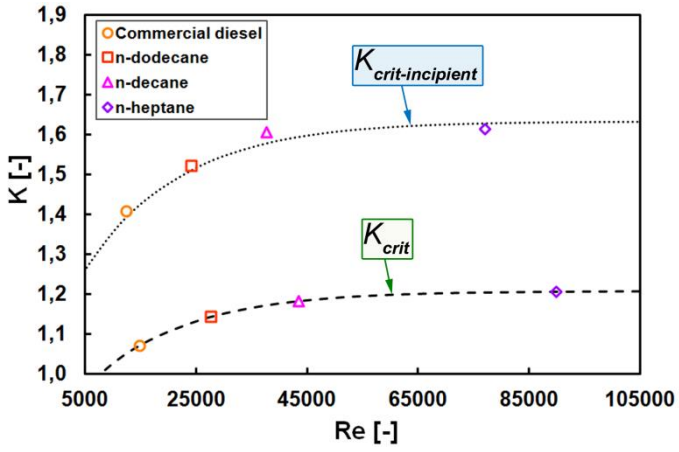

Figure 19. Comparison between K_{crit} and $K_{crit-incipient}$.

5. CONCLUSIONS

The aim of this paper was to know the cavitation behavior in a transparent nozzle carrying out a study to determine the cavitation inception for different fuels. For this purpose special near-nozzle field visualization in a pressurized diesel fuel chamber has been used. Using this facility, as the orifice is injecting in a liquid environment, backlighting technique allows the visualization of cavitation bubbles both inside the orifice and in the spray.

After doing the nozzle geometry characterization and presenting the results from hydraulic characterization and visualization, several conclusions have been obtained:

- When comparing the fuels it can be observed that as the viscosity is less the fuel tends to cavitate sooner. This is due to the fact that viscosity is inversely proportional to the Reynolds number and thus with less viscous fuels higher Reynolds number are obtained at the exit and cavitation appears earlier.
- When plotting the discharge coefficient in function of the Reynolds number it can be seen that all fuel results under non-cavitating conditions are on the same asymptotic tendency line. Besides a correlation could be obtained for the critical cavitation number in function of Reynolds number.
- Mass flow choked has been compared with the incipient cavitation shown in visualization tests for each fuel. In terms of K, the cavitation detection by the optical procedure has shown higher values than those found in mass flow choked. This effect could be due to the fact that there has to exist a big amount of bubbles in the exit section for the mass flow collapse to occur.
- A new cavitation number ($\boldsymbol{K_{crit-incipient}}$) was obtained for each fuel taking into account the incipient cavitation criterion. This incipient cavitation occurs at less critical conditions than the collapse of the mass flow rate for all fuels.
- It could be observed that the flow collapse occurs right when cavitation is fully developed in the orifice. Also, that the first bubbles in the spray appear before the mass flow collapse occurs. This happens with all fuels.
- Finally, the influence of the refractive index of each fuel in the quality of obtained images is observed. This way, since commercial gasoil has the closest refractive index to the transparent nozzle refractive index the images obtained with this fuel have the best quality and as the difference between both refractive index increases images with less quality are obtained.

ACKNOWLEDGMENTS

This work has been funded by Universidad Politécnica de Valencia from Spain, in the framework of the project "Estudio de la influencia del levantamiento de aguja en el proceso de inyeccion diésel", Reference No. PAID-06-10-2362. The authors would like to José Enrique del Rey* for his collaboration in the experimental measurements.

(*) From CMT-Motores Térmicos. Universidad Politécnica de Valencia.

NOMENCLATURE

A, B, C, D	Coefficients from correlations
A_o	Geometrical outlet area
C_c	Nurick contraction coefficient
C_d	Discharge coefficient
D_o	Diameter at the orifice outlet
K	Cavitation number
$\dot{m}$	Mass flux
p_{inj}	Injection pressure
p_{back}	Discharge back pressure
p_v	Vapor pressure
Re	Reynolds number at the nozzle outlet
U_{th}	Theoretical Bernoulli outlet velocity

Greek Symbols

Δp	Pressure drop
ρ_f	Fuel density
ν_f	Kinematic viscosity of the fuel

REFERENCES

1. Soteriou, C., Smith, M., Andrews, R., 1995. Direct injection diesel sprays and the effects of cavitation and hydraulic flip on atomization. SAE Paper 950080.

2. Hiroyasu, H., 2000. Spray breakup mechanism from the hole-type nozzle and its applications. Atomization and Sprays 10, 511–527.

3. Ganippa, L.C., Bark, G., Andersson, S., Chomiak, J., 2004. Cavitation: a contributory factor in the transition from symmetric to asymmetric jets in cross flow nozzles. Experiments in Fluids 36, 627–634.

4. Lee, C.S., Lee, K.H., Reitz, R.D., Park, S.W., 2006. Effect of split injection on the macroscopic development and atomization characteristics of a diesel spray injected through a common-rail system. Atomization and Sprays 16 (5), 543–562.

5. Payri, F., Bermúdez, V., Payri, R., Salvador, F.J., 2004a. The influence of cavitation on the internal flow and the Spray characteristics in diesel injection nozzles. Fuel 83, 419–431.

6. Payri, R., Guardiola, C., Salvador, F.J., Gimeno, J., 2004b. Critical cavitation number determination in diesel injection nozzles. Experimental Techniques 28 (3), 49–52.

7. Payri, R., F.J. Salvador, J. Gimeno, J. de la Morena, 2009. Study of cavitation phenomena based on a technique for visualizing bubbles in a liquid pressurized chamber. International Journal of Heat and Fluid Flow 30 (2009) 768–777.

8. Sou, A., Hosokawa, S., Tomiyama, A., 2007. Effects of cavitation in a nozzle on liquid jet atomization. International Journal of Heat and Mass Transfer 50, 3575–3582.

9. Sou, A. Tomiyama, A. Hosokawa, S. Nigorikawa, S. Maeda, Cavitation in a Two-Dimensional Nozzle and Liquid Jet Atomization, JSME International Journal Series B, 2006.

10. Winklhofer, E., Kull, E., Kelz, E., Morozov, A., 2001. Comprehensive hydraulic and flow field documentation in model throttle experiments under cavitation conditions. ILASS-Europe 2001, Zurich, 2–6 September 2001.

11. Mishra, C., Peles, Y., 2005. Cavitation in flow through a micro-orifice inside a silicon microchannel. Physics of fluids 17, 013601.

12. Oda, T.; Goda, Y.; Kanaike, S.; Aoki, K. & Ohsawa, K. Experimental Study about internal Cavitating Flow and Primary Atomization of a Large-Scaled VCO Diesel Injector with Eccentric Needle 11th Triennial International Annual Conference on Liquid Atomization and Spray Systems, 2009, 132.

13. Ganippa L.C., Bark G., Andersson S., Chomiak J., Comparison of cavitation phenomena in transparent scale-up single-hole diesel nozzles, Proc. CAV2001 (2001) A9.005.

14. Andriotis A. and Arcoumanis C., Influence of vortex flow and cavitation on near-nozzle diesel spray dispersion angle, Atomization and Sprays, 2008.

15. Mitroglou N., Gavaises M., Nouri J.M. and Arcoumanis C. Cavitation inside enlarged and real-size fully transparent injector nozzles and its effect on near nozzle spray formation, DIPSI Workshop 2011 on Droplet Impact Phenomena & Spray Investigation Bergamo, Italy, 2011.

16. Chaves H., Knapp M., Kubitzek A., and Obermeier F., Experimental Study of Cavitation in the Nozzle Hole of Diesel Injectors Using Transparent Nozzles, SAE Paper No. 950290, 1995.

17. Arcoumanis, C., M. Badami, H. Flora, and M. Gavaises, Cavitation in Real-Size Multi-Hole Diesel Injector Nozzles. SAE Paper 2000-01-1249, 2000.

18. Walther J., Schaller J.K., Wirth R., Tropea C., Investigation of internal flow in transparent diesel injection nozzles using fluorescent particle image velocimetry (FPIV), Proc. ICLASS 2000 (2000).

19. Nurick, W.H., 1976. Orifice cavitation and its effect on spray mixing. ASME Journal of Fluids Engineering 222, 681–687.

20. Lichtarowicz, A., Duggins, R.K., Markland, E., 1965. Discharge coefficients for incompressible non-cavitating flow through long orifices. Journal of Mechanical Engineering Science 7 (2).

21. Suh, H.K., Lee, C.S., 2008. Effect of cavitation in nozzle orifice on the diesel fuel atomization characteristics. International Journal of Heat and Fluid Flow 29 (4), 1001–1009.

22. Blessing, M.; König, G.; Krüger, C.; Michels, U. & Schwarz, V. Analysis of flow and cavitation phenomena in diesel injection nozzles and its effects on spray and mixture formation SAE Paper 2003-01-1358, Society of Automotive Engineers, Inc., Warrendale, Pennsylvania, USA, 2003.

23. H. Malitson, "Refractive Index of Fused Silica," J. Opt. Soc. Am. 55, 1205 (1965).

24. Ghosh G., Handbook of Thermo-Optic Coefficients of Optical Materials with Applications Academic, San Diego, Calif., 1997.

Deanesly R.M. and Carleton l.T., Physical Constants of the Normal Paraffin Hydrocarbons. The Journal of Physical Chemistry, ACS Publications, 1941.